

A parametric level-set approach for seismic full-waveform inversion

Kadu, Ajinkya; van Leeuwen, Tristan; Mulder, Wim

DOI

[10.1190/segam2016-13870276.1](https://doi.org/10.1190/segam2016-13870276.1)

Publication date

2016

Document Version

Accepted author manuscript

Published in

SEG Technical Program Expanded Abstracts 2016

Citation (APA)

Kadu, A., van Leeuwen, T., & Mulder, W. (2016). A parametric level-set approach for seismic full-waveform inversion. In C. Sicking, & J. Ferguson (Eds.), *SEG Technical Program Expanded Abstracts 2016* (pp. 1146 - 1150). (SEG Technical Program Expanded Abstracts; Vol. 2016). SEG.
<https://doi.org/10.1190/segam2016-13870276.1>

Important note

To cite this publication, please use the final published version (if applicable).
Please check the document version above.

Copyright

Other than for strictly personal use, it is not permitted to download, forward or distribute the text or part of it, without the consent of the author(s) and/or copyright holder(s), unless the work is under an open content license such as Creative Commons.

Takedown policy

Please contact us and provide details if you believe this document breaches copyrights.
We will remove access to the work immediately and investigate your claim.

A Parametric Level-Set Approach for Seismic Full-Waveform Inversion

Ajinkya Kadu* and Tristan van Leeuwen, Mathematical Institute, Utrecht University

Wim A. Mulder, Delft University of Technology & Shell Global Solutions International B.V.

SUMMARY

In seismic exploration, the delineation of large bodies with hard exterior contrasts but nearly constant interior properties is a challenge. Examples include salt diapirs, salt slabs, anhydrite or basalt layers. Salt geometries are of particular interest because they often have hydrocarbon reservoirs on their sides or underneath. This paper introduces a parametric level-set method for the reconstruction of such geometries in seismic full-waveform inversion (FWI). The level-set determines the outline of the salt geometry and evolves during the inversion in terms of its underlying parameters. For the latter, we employ Gaussian radial basis functions that can represent a large class of shapes with a small number of parameters. This keeps the dimensionality of the inverse problem small, which makes it easier to solve. First tests on a simple 2-D square box model show dramatic improvements over classic FWI.

INTRODUCTION

Full-waveform inversion attempts to obtain detailed estimates of subsurface medium parameters by fitting observed seismic data to modeled data. The absence of usable low-frequency data can make the reconstruction of large-scale variations extremely difficult. Tomographic methods, such as traveltime tomography (TT) or migration velocity analysis (MVA), can fill in the spectral gap to some extent. However, these methods are often based on the assumption that the model parameters can be separated in a smoothly varying *background* velocity and an oscillatory *reflectivity* component. Based on either diving waves or reflected events, TT and MVA can retrieve the smooth background. Migration subsequently retrieves the reflectivity. FWI bridges the gap between velocity estimation and migration to some extent, but still needs a kinematically accurate background model to start with.

When the separation-of-scale assumption is violated, traditional velocity estimation methods break down. To overcome this issue, several non-linear extensions of conventional MVA have been proposed (Symes, 2008; Biondi and Almomin, 2013). Although these approaches promise to address the ill-posedness of FWI, they are computationally very demanding.

A particularly relevant setting in which the separation-of-scales argument fails to hold is in the presence of strong contrasts, such as salt diapirs, salt slabs, anhydrite or basalt layers. Salt geometries are of particular interest because they often have hydrocarbon reservoirs on their sides or underneath. In these settings, it is reasonable to assume that the subsurface can be described as one or more continuous bodies (salt) with known constant material parameters, surrounded by continuously varying parameters (sediment). Such prior knowledge is very powerful and can help overcome issues with ill-posedness and miss-

ing data (Hansen, 1998; Asnaashari et al., 2013; Esser et al., 2016). In this abstract we describe the use of a level-set approach to represent such bodies and cast the inversion in terms of its underlying parameters.

THEORY

The classical least-squares formulation of FWI (Virieux and Operto, 2009) is defined as

$$\min_m \left\{ f(m) := \frac{1}{2} \|F(m) - d\|_2^2 \right\}, \quad (1)$$

where $m(x) \in \mathcal{M}$ is the spatially varying model parameter (e.g., the sound speed), $F : \mathcal{M} \rightarrow \mathcal{D}$ is the forward modeling operator that maps from the model space \mathcal{M} to the data space \mathcal{D} , and d represents the observed data.

The optimization problem (1) is typically solved using a Newton-like algorithm (Pratt et al., 1998) as

$$m^{(k+1)} = m^{(k)} - \lambda_k H_k^{-1} \nabla f(m^{(k)}),$$

where λ_k is the step size and H_k denotes (an approximation of) the Hessian of f at iteration k . The gradient of the objective is given by

$$\nabla f(m) = J(m)^*(F(m) - d),$$

where $J(m)$ is the Jacobian of F and J^* denotes its adjoint.

The ill-posedness of the problem requires regularization. We distinguish two types: *implicit* regularization, where we add a penalty $\rho(m)$ to the objective in (1) such that $\rho(m) \approx 0$ when $m \in \mathcal{M}$, or *explicit* regularization, where we expand m in an appropriate basis. For example, when we expect the model to vary smoothly, we may choose a representation of the form

$$m(x) = \sum_{i=1}^n m_i \phi_i(x),$$

where $\phi_i(x)$ are smooth basis functions, such as B-splines. Alternatively, we can add a penalty term that penalizes the derivatives of m , e.g., $\rho(m) = \|\nabla m\|_2^2$ with ∇ the gradient operator. Such a regularization is motivated by a separation-of-scales argument. Indeed, when the scales of the model are separable, we can invert for a smoothly varying velocity from low-pass filtered data (Bunks et al., 1995).

In some geological settings, however, the scales do *not* separate, and we need to find an alternative form of regularization. In case we expect our model to have strong discontinuities, a popular choice is a Total-Variation (TV) regularization with $\rho(m) = \|\nabla m\|_1$ (Rudin et al., 1992; Lin and Huang, 2014). A disadvantage is that such a regularization acts globally and induces the model to be blocky everywhere.

A Parametric Level-Set for Full-Waveform Inversion

In this paper, we propose a mixed representation for the particular case of salt bodies. We represent m as

$$m(x) = \begin{cases} m_1 & \text{if } x \in \Omega, \\ m_0(x) & \text{otherwise.} \end{cases}$$

Here, Ω indicates the salt-body, m_1 is the constant value of the model parameter inside the salt body and $m_0(x)$ denotes the spatially varying parameters in the sediment. It is not straightforward to come up with a penalty term that promotes such structure on m , but we can represent the model explicitly as

$$m(x) = [1 - a(x)]m_0(x) + a(x)m_1,$$

where $a(x) \in \{0, 1\}$ is an indicator function given by

$$a(x) = \begin{cases} 1 & \text{if } x \in \Omega, \\ 0 & \text{otherwise.} \end{cases}$$

Figure 1 sketches three different models, representing the smooth variation, blocky structure and a combination of both. Model 1 typically refers to the sediment structure, while model 2 represents the salt geometry. We generally expect a seismic velocity distribution similar to model 3, combining model 1 & 2.

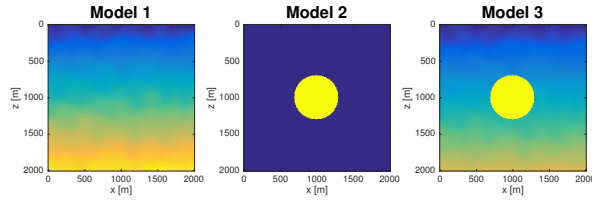


Figure 1: Model 1: smooth velocity variation (sediment). Model 2: circular blob with higher velocity (salt). Model 3: combination of smooth variation and blocky model.

The inverse problem now consists in finding the set Ω — or equivalently, the indicator function $a(x)$ — and the model parameters $m_0(x)$ and m_1 . Because of the requirement that $a \in \{0, 1\}$, this is a combinatorial optimization problem. Although efficient (heuristic) algorithms exist for such problems (Batenburg and Sijbers, 2007), we choose a different route and represent a with a level-set function.

Level-set method

The basic idea behind level-set methods is to represent the boundary of the domain Ω as the zero contour of a level-set $\phi(x)$. The domain itself is then defined by $\Omega = \{x | \phi(x) \geq 0\}$ and negative values of $\phi(x)$ corresponds to points outside Ω (Osher and Fedkiw, 2001). This then leads us to represent the indicator function as $a(x) = h(\phi(x))$, where h is the Heaviside function. Figure 2 shows three examples of a level-set function and its corresponding domain Ω .

We now express the model as

$$m(x) = m_0(x)[1 - h(\phi(x))] + m_1 h(\phi(x)).$$

Depending on the regularity of Ω , we can impose additional smoothness constraints on ϕ . The conventional level-set method

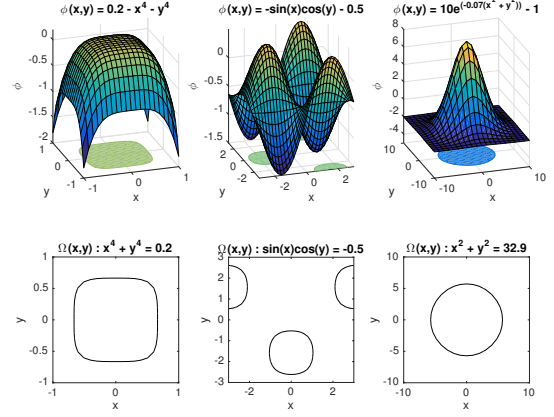


Figure 2: level-set functions and corresponding Ω

now aims to find a function ϕ such that the corresponding model parameters explain the data, i.e. $F(m_0(x)[1 - h(\phi(x))] + m_1 h(\phi(x))) \approx d$. (Burger, 2001; Dorn and Lesselier, 2006). In order to be able to compute sensitivities of the objective function with respect to ϕ , we need to differentiate the Heaviside function, yielding $h'(x) = \delta(x)$ with δ the Dirac delta function. For numerical computations, it is more convenient to introduce a smooth approximation of the Heaviside function, for example,

$$h_\varepsilon(x) = \frac{1}{2} \left[1 + \frac{2}{\pi} \arctan\left(\frac{\pi x}{\varepsilon}\right) \right].$$

Figure 3 shows an example of the Heaviside function and its smooth approximation.

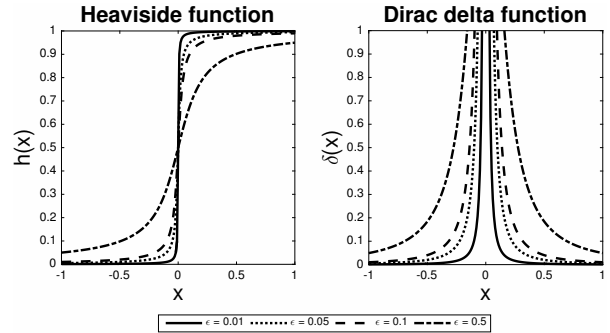


Figure 3: Heaviside and corresponding smoothed Dirac delta function for various ε

The level-set method was originally introduced for tracking regions in fluid flow applications, providing a natural way to evolve the level-set by solving a Hamilton-Jacobi equation (Osher and Sethian, 1988). In applications like FWI, it is not obvious how to update the level-set away from the boundary of the domain, because $h'_\varepsilon(x)$ quickly tends to zero. To address this issue, we follow Aghasi et al. (2011) and parametrize the level-set function using n terms as

$$\phi(x) = \sum_{i=1}^n \alpha_i \Psi(\|\beta_i(x - \chi_i)\|_2),$$

A Parametric Level-Set for Full-Waveform Inversion

where χ_i are the nodes, β_i is a scaling factor, α_i are the weights and Ψ is a radial basis function (RBF), e.g., $\Psi(r) = \exp(-r^2)$. We can now express the inverse problem, for fixed m_0 and m_1 , as

$$\min_{\alpha} \left\{ g(\alpha) := \|F(m(x, \alpha)) - d\|_2^2 \right\}, \quad (2)$$

where $m(x, \alpha) = m_0(x)[1 - h_\varepsilon(\phi(x; \alpha))] + m_1 h_\varepsilon(\phi(x; \alpha))$. The gradient of g with respect to the weights is readily computed with the chain rule;

$$\frac{\partial g}{\partial \alpha_i} = \langle \nabla f, (m_1 - m_0) h'_\varepsilon(\phi) \Psi(\|\beta_i(\cdot - \chi_i)\|) \rangle, \quad (3)$$

where $\langle \cdot, \cdot \rangle$ denotes the inner product. Because of the infinite support of the radial basis functions, each basis function contributes to the definition of the boundary. Hence, the derivative $\frac{\partial g}{\partial \alpha_i}$ will never vanish, unless we are at a (local) minimum where $\nabla f = 0$. An added benefit of this parametrization over the conventional level-set method is that the dimensionality is greatly reduced. Instead of having a finely gridded function ϕ as unknown, we now have only n unknowns. This formulation further opens up the possibility for adaptive refinement by optimizing over the location of the nodes χ_i and scale factors β_i . We can readily solve the optimization problem (2) using a gradient-based method.

EXAMPLES

To demonstrate the feasibility of the parametric level-set approach, we present two numerical experiments. First, we show that complicated salt bodies can be represented accurately using a single parametric level-set function. Then, we show how the level-set approach can be used to effectively retrieve a square anomaly in a smooth background. In the following examples, the centers (χ) and scaling factors (β) are kept fixed. The scaling factors are chosen in accordance with the spacing between the nodes χ_i to produce reasonable overlap between neighboring RBFs.

SEAM Model

As a first step, we demonstrate the reconstruction of a salt body on the 2-D SEAM model (Fehler and Keliher, 2011) as a pure imaging problem, without seismic data. Figure 4 displays the velocity model with two salt bodies, having a velocity of 4800 m/s. The wave speed varies from 1490 m/s to 4800 m/s in the sediment. The model is discretized on a grid of 876×756 points with a grid spacing of 20 m in x and 10 m in z . We abstract the salt body image, $a(x)$, from the velocity model by assigning a value of 1 to the salt and 0 elsewhere. To find the corresponding level-set function, we solve the following least-squares problem

$$\min_{\alpha \in \mathbb{R}^n} \|h_\varepsilon(\phi(x; \alpha)) - a\|_2^2,$$

using a standard Quasi-Newton method. A total of $n = 600$ Gaussian RBFs with $\beta_i = 5 \times 10^6$ are spread equidistantly over the model grid to parametrize the level-set function. The dimensionality is reduced by a factor of 10^3 in this case. Figure 5 shows the recovered salt geometry after 200 iterations.

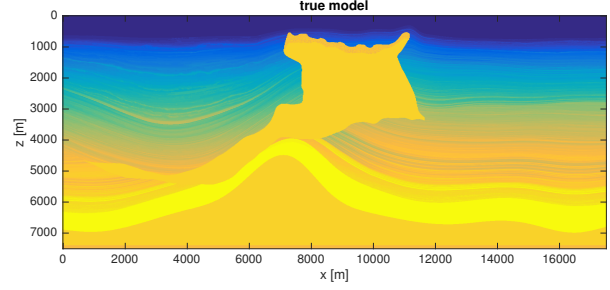


Figure 4: True velocity distribution of 2-D SEAM model

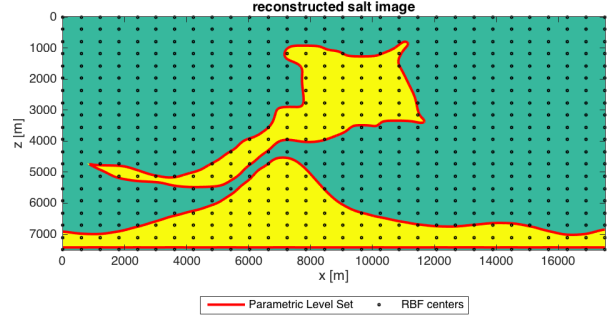


Figure 5: recovered salt geometry

Full-waveform inversion

As the next step, we test FWI, in combination with the parametric level-set method as a penalty term, on the simple but non-trivial model depicted in Figure 6. The background velocity increases linearly with depth from 2400 m/s to 2500 m/s. The square anomaly has a constant velocity of 3000 m/s. The model is defined on a 2000 m by 2000 m grid with a grid spacing of 10 m in both directions. The basement reflector is included to produce a more favorable setting for waveform inversion. Note, however, that the reflector is *not* present in the initial model. We synthetically generate the observed data with 20 sources and 100 receivers placed at top of the model, over a range of 4–16 Hz with a spacing of 0.2 Hz using a frequency-domain finite difference code.

The objective is optimized with respect to the weights α only, keeping the nodes, scaling factors, and the parameters $m_0(x)$ and m_1 fixed at their true value. We invert the data using a multi-scale approach in 6 batches: [4–6], [6–8], ..., [14–16], with 10 frequencies each. The optimization is performed by a Quasi-Newton method, L-BFGS, with 100 iterations per frequency batch.

The initial model for conventional FWI is the background model. Figure 7 shows the reconstructed model. The result predicts the upper and lower surface of the anomaly to some extent but fails to identify its proper shape. The basement reflector is reconstructed to some extent, but is curved upward in the center, indicating a failure to correctly identify the velocity of the anomaly.

For the parametric level-set approach, we use 400 Gaussian RBFs with $\beta = 10^{-4}$, spread over the model grid as shown in

A Parametric Level-Set for Full-Waveform Inversion

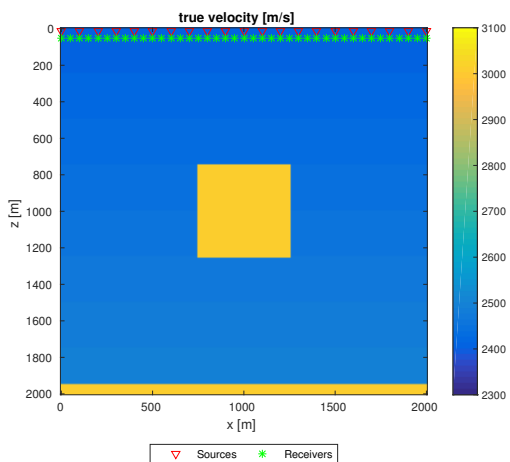


Figure 6: True velocity of the model with sources and receivers at the top

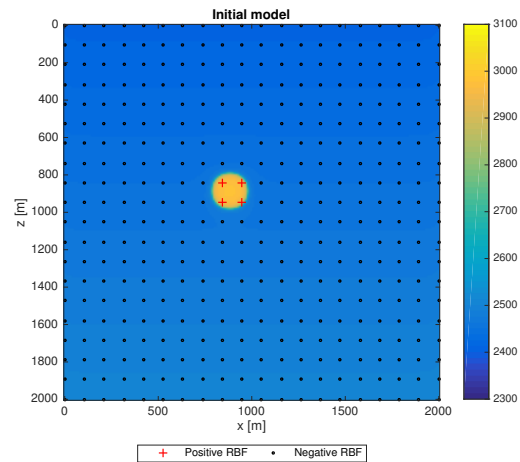


Figure 8: Initial model for the parametric level set with RBF centers

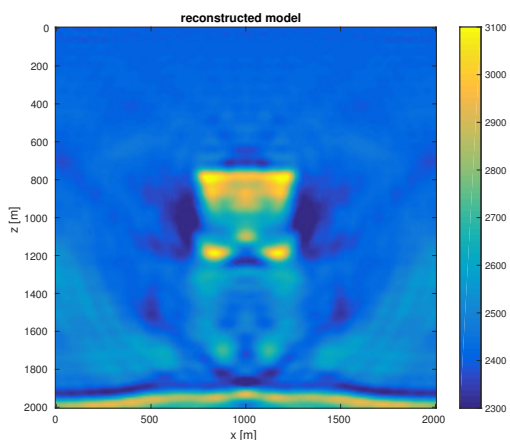


Figure 7: Reconstructed model from classic FWI without the level-set approach

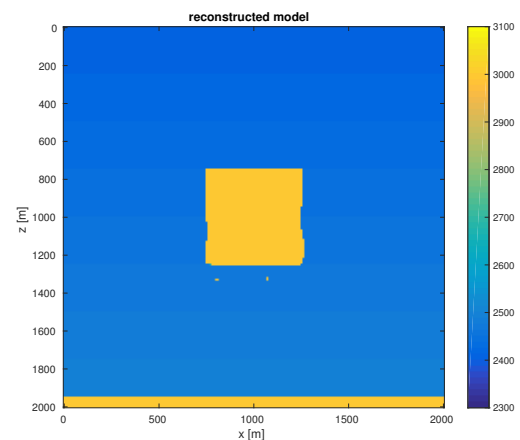


Figure 9: Reconstructed model from FWI with the parametric level-set approach

Figure 8. The background velocity, m_0 , is the true background velocity. All the RBFs have been initialized with negative weights ($\alpha_i = -1$) except the 4 RBFs in the center ($\alpha_i = 1$), as shown in Figure 8. Figure 9 presents the model obtained by FWI together with the parametric level-set method. We see that the level-set approach is able to almost perfectly reproduce both the anomaly and the basement reflector.

CONCLUSIONS

We presented the application of the parametric level-set method to full-waveform inversion and salt geometry determination. A small number of Gaussian radial basis function suffice to approximate the level set of a complex salt geometry, leading a large reduction of the problem's dimensionality and an intrinsic regularization of the problem. We successfully demonstrated the capability of the method by image reconstruction of a complex body, using the level-set representation by itself, as well as by full-waveform inversion on a simple but non-trivial

model, using both the least-squares data misfit and the level-set representation.

ACKNOWLEDGMENTS

This work is part of the Industrial Partnership Programme (IPP) 'Computational sciences for energy research' of the Foundation for Fundamental Research on Matter (FOM), which is part of the Netherlands Organisation for Scientific Research (NWO). This research programme is co-financed by Shell Global Solutions International B.V. The second author is financially supported by the Netherlands Organisation of Scientific Research (NWO) as part of research programme 613.009.032. The first author was further supported by an NDNS travel grant. The first two authors are grateful to Felix Herrmann for offering hospitality, computational resources and a stimulating research environment. They thank Eldad Haber for stimulating discussions and pointing out the applicability of the parametric level-set method.

A Parametric Level-Set for Full-Waveform Inversion

REFERENCES

- Aghasi, A., M. Kilmer, and E. L. Miller, 2011, Parametric level set methods for inverse problems: *SIAM Journal on Imaging Sciences*, **4**, 618–650.
- Asnaashari, A., R. Brossier, S. Garambois, F. Audebert, P. Thore, and J. Virieux, 2013, Regularized seismic full waveform inversion with prior model information: *GEOPHYSICS*, **78**, R25–R36.
- Batenburg, K., and J. Sijbers, 2007, Dart: A Fast Heuristic Algebraic Reconstruction Algorithm for Discrete Tomography: 2007 IEEE International Conference on Image Processing, IEEE, IV – 133–IV – 136.
- Biondi, B., and A. Almomin, 2013, Tomographic full-waveform inversion (TFWI) by combining FWI and wave-equation migration velocity analysis: *The Leading Edge*, **32**, 1074–1080.
- Bunks, C., F. M. Saleck, S. Zaleski, and G. Chavent, 1995, Multiscale seismic waveform inversion: *GEOPHYSICS*, **60**, 1457–1473.
- Burger, M., 2001, A level set method for inverse problems: *Inverse problems*, **17**, 1327.
- Dorn, O., and D. Lesselier, 2006, Level set methods for inverse scattering: *Inverse Problems*, **22**, R67.
- Esser, E., L. Guasch, F. J. Herrmann, and M. Warner, 2016, Constrained waveform inversion for automatic salt flooding: *The Leading Edge*, **35**, 235–239.
- Fehler, M., and P. J. Keliher, 2011, SEAM Phase 1: Challenges of Subsalt Imaging in Tertiary Basins, with Emphasis on Deepwater Gulf of Mexico: Society of Exploration Geophysicists.
- Hansen, P. C., 1998, Rank-Deficient and Discrete Ill-Posed Problems: Society for Industrial and Applied Mathematics.
- Lin, Y., and L. Huang, 2014, Acoustic- and elastic-waveform inversion using a modified total-variation regularization scheme: *Geophysical Journal International*, **200**, 489–502.
- Osher, S., and R. P. Fedkiw, 2001, Level set methods: an overview and some recent results: *Journal of Computational physics*, **169**, 463–502.
- Osher, S., and J. A. Sethian, 1988, Fronts propagating with curvature-dependent speed: algorithms based on hamilton-jacobi formulations: *Journal of computational physics*, **79**, 12–49.
- Pratt, R. G., C. Shin, and G. Hick, 1998, Gauss-newton and full newton methods in frequency-space seismic waveform inversion: *Geophysical Journal International*, **133**, 341–362.
- Rudin, L. I., S. Osher, and E. Fatemi, 1992, Nonlinear total variation based noise removal algorithms: *Physica D: Nonlinear Phenomena*, **60**, 259–268.
- Symes, W. W., 2008, Migration velocity analysis and waveform inversion: *Geophysical Prospecting*, **56**, 765–790.
- Virieux, J., and S. Operto, 2009, An overview of full-waveform inversion in exploration geophysics: *Geophysics*, **74**, WCC1–WCC26.